

Article

A Novel PETG Microchannel Reactor for Microwave-Powered Biodiesel Production

Koguleshun Subramaniam ¹, Kang Yao Wong ¹, Kok Hoe Wong ¹ , Cheng Tung Chong ²  and Jo-Han Ng ^{1,*}

¹ Carbon Neutrality Research Group, University of Southampton Malaysia, Iskandar Puteri 79100, Malaysia; k.subramaniam@soton.ac.uk (K.S.); drmatthewwky@gmail.com (K.Y.W.); k.h.wong@soton.ac.uk (K.H.W.)

² China-UK Low Carbon College, Shanghai Jiao Tong University, Lingang, Shanghai 201306, China; ctchong@sjtu.edu.cn

* Correspondence: j.ng@soton.ac.uk

Abstract: Biodiesel stands at the forefront as a replacement for fossil diesel in compression ignition engines, particularly in the transportation sector where diesel engines are the primary movers. However, biodiesel production is hampered by poor heat and mass transfer during the transesterification reaction, leading to long production times and high costs due to inefficient energy utilisation. This study targets heat and mass transfer issues during the production of biodiesel via a synergic approach that combines microwave-assisted heating and microfluidics via a polyethylene terephthalate glycol (PETG) microchannel reactor. The transesterification reaction of palm oil and methanol was investigated using a full factorial design of experiments (DOE) method. Biodiesel yield was quantified via gas chromatographic analysis, and the results were optimised using statistical analysis. Optical analysis of slug quantification within the microchannel revealed that small slugs, smaller than 1 mm, accelerated the transesterification reaction. The composite-optimised experimental results, aimed at minimising energy costs and environmental impacts while maximising fatty acid methyl ester (FAME) yield, indicate a reaction temperature of 50 °C, a catalyst loading of 1.0 wt.%, and a 3:1 methanol to oil molar ratio. Regression analysis revealed that the reaction temperature was statistically insignificant when utilising the PETG microchannel reactor. This key finding positively impacts biodiesel production as it relates to significantly reduced energy intensity, costs, and emissions. Overall, this research work paves a pathway toward an energy-efficient and sub-minute rapid transesterification reaction, highlighting the effectiveness of microwave heat delivery and effects of microfluidics via the PETG microchannel reactor in overcoming heat and mass transfer barriers in biodiesel production.

Keywords: biodiesel; PETG microchannel reactor; transesterification reaction; microfluidics; microwave heating



Citation: Subramaniam, K.; Wong, K.Y.; Wong, K.H.; Chong, C.T.; Ng, J.-H. A Novel PETG Microchannel Reactor for Microwave-Powered Biodiesel Production. *Energies* **2024**, *17*, 2103. <https://doi.org/10.3390/en17092103>

Academic Editor: Bruno Zelić

Received: 14 February 2024

Revised: 7 April 2024

Accepted: 11 April 2024

Published: 28 April 2024



Copyright: © 2024 by the authors. Licensee MDPI, Basel, Switzerland. This article is an open access article distributed under the terms and conditions of the Creative Commons Attribution (CC BY) license (<https://creativecommons.org/licenses/by/4.0/>).

1. Introduction

Fossil fuels, with their utilisation up to 82% in 2022, dominate the energy scenario to fulfil the global energy demand [1]. Nevertheless, the current utilisation of fossil fuels anticipates depletion, while its combustion releases hazardous emissions into the environment in the form of greenhouse gases (GHGs) [2]. Biodiesel is a liquid biofuel that strives to be a suitable and ‘green’ replacement for fossil fuels. This is because biodiesel can be produced, utilised, and stored while maintaining the pre-existing petroleum infrastructure of today [3]. Particularly within the context of compression ignition engines, the utilisation of biodiesel is feasible without engine modifications [4]. In addition, biodiesel shares similar physical and chemical properties as fossil diesel, thus eliminating compatibility issues [5].

However, industrial biodiesel production through the transesterification reaction in commercial reactors faces heat and mass transfer limitations. This translates to slow reaction time beyond one hour due to poor reaction kinetic rates [6]. Transesterification occurs at the interface between oil and alcohol, which are the reactants for biodiesel production. The

limitations of heat and mass transfer are significant, since oil and alcohol are naturally immiscible [7]. This necessitates stirring of the reaction mixture to lower the mass transfer limitation, hence increasing the rate of biodiesel conversion [8]. Nevertheless, the vigorous mechanical stirring incurs high energy demand. Moreover, the cost of biodiesel production has increased from about 68% to 85% of the feedstock cost from the mid 1990s to current times [9]. Thus, technologies to enhance the efficiency of transesterification for a rapid reaction in the absence of heat and mass transfer limitations is crucial to maintain the sustainability of biodiesel production and utilisation.

Microchannel reactors are known to enable rapid reactions and facilitate efficient heat and mass transfer to reactants for reactive flow processes, such as biodiesel production. This is achieved by benefiting from the high surface area to volume ratio of the microchannels. In contrast to conventional batch reactors, microchannel reactors enable continuous flow transesterification reaction that maximise biodiesel yield, while allowing better control over the reaction parameters [10].

Yue et al. [11] reported a biodiesel production study using soybean oil in a micro-fixed-bed microchannel reactor having an internal diameter of 2 mm. The reaction conditions of transesterification were maintained at a reaction temperature of 70 °C and methanol to oil molar ratio of 12:1. A biodiesel yield of 99.4% was obtained at about 8 min of reaction time. Also, a 94% mixing index of reactants was achieved at a reactor length of 25 mm, induced by the twisted flow pattern and geometric obstruction within the microchannel reactor. The study suggested the utilisation of microchannel reactors for an energy-conserving, environmentally sound, and continuous flow production of biodiesel.

Pavlovic et al. [12] investigated biodiesel production in a Teflon microchannel reactor having a length of 800 mm and internal diameter of 0.8 mm. Transesterification was carried out using sunflower oil, catalysed using a base catalyst obtained from waste chicken eggshell. The efficiency of biodiesel production in the microchannel reactor was contrasted against a traditional batch reactor. A 32.6% higher biodiesel yield was revealed in the microchannel reactor within 10 min of reaction time, compared to the batch reactor.

An investigation by Laziz et al. [13] indicated the ability of microchannel reactors to enhance the mass transfer of reactants for biodiesel production by escalating its mixing effects. In comparison with experimental results, a computational fluid dynamics (CFD) simulation was utilised to investigate the mixing pathway of reactants within a cross-junction microchannel reactor. The findings suggested that the enhanced ratio of the reactor's surface area to volume induced a slug flow pattern. Mixing of oil and alcohol was enhanced by the formation of vortices within the slugs. A slow reactant flow rate was found to enhance the formation of slugs. Meanwhile, fast flow rates during the slug-moving phase resulted in elevated mixing of reactants due to the escalated vortex velocity within the slugs. Both of these phases facilitated enhanced mass transfer in the transesterification reaction.

Microwaves are short electromagnetic waves produced by the conversion of electrical energy, typically emitted by a magnetron. Microwave-assisted transesterification has been explored by researchers for rapid and energy efficient biodiesel production. Microwave-assisted heating is the transmission of microwave energy in the form of irradiation to elevate the internal energy of reactant molecules. Significant energy savings and a reduction in reaction time of up to 60% is reportedly achievable through microwave-assisted biodiesel production, in comparison to conventional heating via conduction [14].

Buasri et al. [15] investigated microwave-assisted biodiesel production of waste cooking oil, catalysed by a sulfonated palm seed cake catalyst. The experimental work was optimised using machine learning and Box–Behnken design to predict the highest biodiesel yield. A 98.62% biodiesel yield was indicated under optimised reaction conditions of catalyst loading of 4.94 wt.% and methanol to oil molar ratio of 16.76:1. Although microwave heating accelerated the transesterification reaction, the reaction time was 8.13 min due to the acid-catalysed process.

Lin et al. [16] investigated a continuous flow production of biodiesel through microwave heating using waste soybean oil. The initial heating phase was achieved within

2 min to attain an average starting temperature of 60.5 °C with 560 W of microwave power. The microwave-assisted transesterification was carried out at a microwave power of 560 W and methanol to oil molar ratio of 3:1. A 95% biodiesel yield was obtained within a short 30 s reaction time. In comparison with conventional heating via hot plate, the energy consumption of microwave-assisted heating reportedly decreased by 93%.

Hsiao et al. [17] investigated sodium hydroxide-catalysed microwave-assisted transesterification using waste cooking oil. A biodiesel conversion of 98.2% was achieved at a 2 min reaction time with 600 W of microwave power to maintain the reaction temperature at 65 °C. Other reaction parameters included a methanol to oil molar ratio of 12:1 and catalyst loading of 0.8 wt.%. In this study, a reaction temperature of 65 °C was found to be best suited for biodiesel production via microwave irradiation, while elevation of the biodiesel conversion rate was insensitive to further increases in other reaction parameters. Despite the increasing number of investigations on microchannel reactors and microwave heating for biodiesel production, studies interactively combining these technologies through a systematic statistical outlook are inadequate.

Hence, this work investigates the synergy between microfluidics and microwave heating technologies to fundamentally understand and overcome the limitations of heat and mass transfer in the transesterification reaction. The performance of a polyethylene terephthalate glycol (PETG) microchannel reactor was evaluated for palm biodiesel synthesis through microwave irradiation heating. The fundamental outcome of this lab-scale study is postulated to be beneficial with regards to biodiesel production time, energy, and affordability when adopted into industrial production processes.

2. Experimental Methodology

This segment discusses the experimental procedures, including materials, manufacturing of the PETG microchannel reactor, setup of the experiment for microwave-assisted biodiesel production, design of the experiment, sample characterisation, and results analysis.

2.1. Materials and Equipment

Sodium hydroxide pellets (99%, Merck, Darmstadt, Germany), methanol (Merck, Darmstadt, Germany), hydrochloric acid (37%, VWR Chemicals, Fontenay-sous-Bois, France), and palm oil (Vesawit, Ipoh, Malaysia) were among the chemicals used in the experimental study. Gas chromatography sample characterisation was carried out using methyl heptadecanoate (analytical standard, Sigma-Aldrich, Buchs, Switzerland) and N-heptane (99% AR grade, QReC, Rawang, Malaysia). Copolyester sheets of polyethylene terephthalate glycol (PETG) were acquired from RS Components Ltd. (Corby, UK).

2.2. Methods

2.2.1. Manufacturing of PETG Microchannel Reactor

The PETG sheets of 6 mm thickness were machined to 100 mm by 150 mm dimensions, forming single plates. The fabrication of the microchannel reactor involved the fusing of two separate plates (i.e., front plate and back plate), as shown in Figure 1. A microchannel length of 1.6 m and a depth of 1 mm were formed on the back plate through etching with a FLUX Beamo CO₂ laser cutter. The back plate was formed by machining through holes at the inlet and outlet openings. The microchannel reactor was subsequently formed by fusing the front and rear plates together using a heat press (Maikesub, Yiwu, China), which was operated for 17 min at 98 °C. Lastly, luers were affixed to the inlet and outlet points using X2000 weld glue structural epoxy adhesive.

PETG was explicitly selected to build the microchannel reactor. This is because PETG is recognised for its exceptional characteristics, including transparency, high chemical resistance, ability to be etched with a laser cutter, easy fusion with a heat press, and inertness to microwave radiation [18]. Microwave-assisted biodiesel production in a microchannel reactor was made possible by taking advantage of PETG's unique material characteristics.

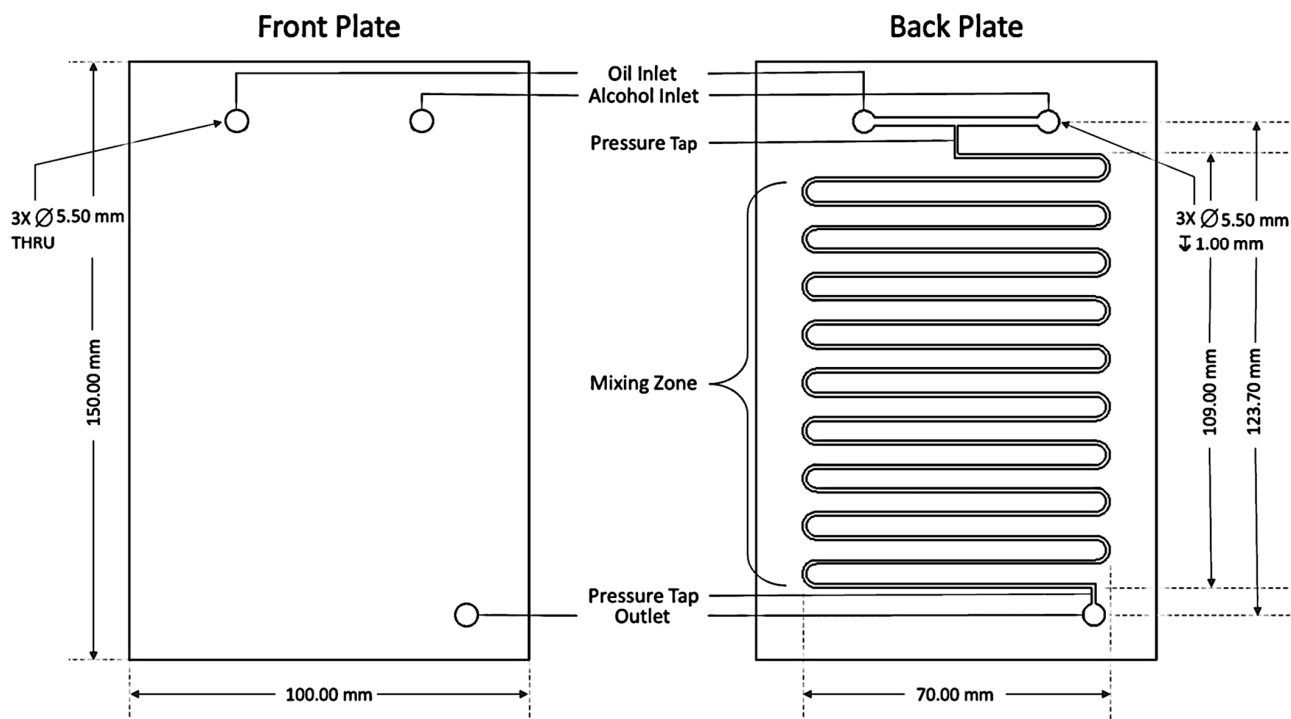


Figure 1. PETG microchannel reactor.

2.2.2. Experimental Setup for Microwave-Assisted Biodiesel Production

Figure 2 illustrates the experimental configuration that was used to carry out the transesterification reaction in a Sharp R207EK household microwave oven. Peristaltic pumps were used to channel the reactants into the PETG microchannel reactor. The pumps were controlled at the required flow rates and all connections for reactant flow were made using silicone tubing. The reactants used were palm oil and sodium methoxide, contained in different vessels. Prior to the transesterification reaction, methoxide solution was prepared in accordance with the relevant alcohol to oil molar ratio by dissolving the required weight of sodium hydroxide catalyst in methanol. Sample collection vials were placed at the outlet point of the microchannel reactor for collection of the post-transesterification products.

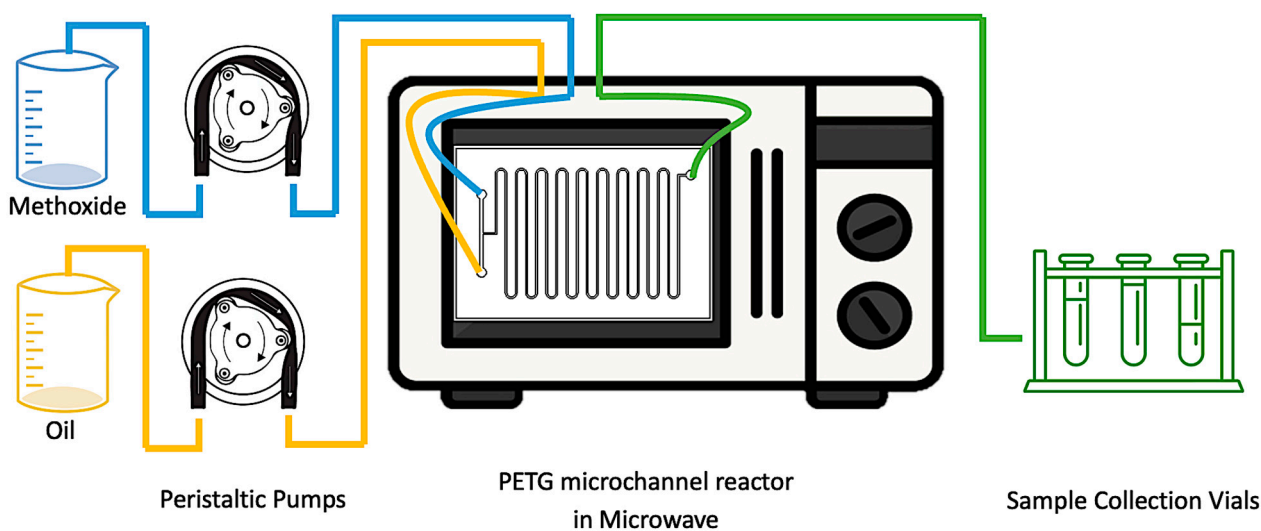


Figure 2. Experimental setup for the production of biodiesel using the PETG microchannel reactor via microwave irradiation heating.

Throughout the transesterification reaction, a steady flow of reactants was maintained by switching on the peristaltic pumps. The surface temperature of the PETG reactor was measured using a Bosch thermal detector at regular intervals and was recorded as the reaction temperature. The power on and power off cycles of the microwave were independently controlled via an external temperature controller as a function of time to maintain and manipulate the desired reaction temperature within an acceptable range. The starting temperature was achieved by turning on the microwave for 3 s and turning it off for 1 s (3:1) in an actively alternating order until the desired reactor surface temperature was achieved. During transesterification, the external controller actively varied the microwave power at a 1 s power on/1 s power off (1:1) cycle. The (1:1) on/off power cycle was found to be the ideal permutation in this study, as other permutations led to overheating failure of the PETG reactor.

The reaction time of the transesterification reaction was 1 min, after which the post-transesterification products were collected in the sample collection vials pre-filled with dilute hydrochloric acid. The instantaneous biodiesel yield was quantified as a function of time through acid quenching, as it halted further transesterification by neutralising the base catalyst.

2.2.3. Design of Experiment

Full factorial design of experiments (DOE) was utilised for microwave-heated biodiesel production in the PETG microchannel reactor. Three different factors were studied, each with three levels, and a total of 27 experimental cases were carried out. Table 1 shows the full factorial DOE incorporating the factors investigated, along with their respective levels of high (1), medium (0), and low (−1).

Table 1. Full factorial design of experiments (DOE) model incorporating experimental factors and levels.

Case No.	Coded Factors with Levels			Uncoded Factors with Levels		
	Methanol to Oil Molar Ratio	Catalyst Loading (wt.%)	Reaction Temperature (°C)	Methanol to Oil Molar Ratio	Catalyst Loading (wt.%)	Reaction Temperature (°C)
1	−1	−1	−1	3	0.6	50
2	−1	−1	0	3	0.6	60
3	−1	−1	1	3	0.6	70
4	−1	0	−1	3	0.8	50
5	−1	0	0	3	0.8	60
6	−1	0	1	3	0.8	70
7	−1	1	−1	3	1	50
8	−1	1	0	3	1	60
9	−1	1	1	3	1	70
10	0	−1	−1	6	0.6	50
11	0	−1	0	6	0.6	60
12	0	−1	1	6	0.6	70
13	0	0	−1	6	0.8	50
14	0	0	0	6	0.8	60
15	0	0	1	6	0.8	70
16	0	1	−1	6	1	50
17	0	1	0	6	1	60
18	0	1	1	6	1	70
19	1	−1	−1	9	0.6	50
20	1	−1	0	9	0.6	60
21	1	−1	1	9	0.6	70
22	1	0	−1	9	0.8	50
23	1	0	0	9	0.8	60
24	1	0	1	9	0.8	70
25	1	1	−1	9	1	50
26	1	1	0	9	1	60
27	1	1	1	9	1	70

The first factor was the reaction temperature ($^{\circ}\text{C}$), at levels of 50, 60, and 70 $^{\circ}\text{C}$. Typically, boiling of methanol is known to adversely influence the transesterification reaction. Hence, the highest reaction temperature was maintained at 70 $^{\circ}\text{C}$, close to the boiling point of methanol. The second factor was the methanol to oil molar ratio, with 3:1, 6:1, and 9:1 being the levels investigated. The lowest methanol to oil molar ratio was maintained at 3:1 for prevention of the reverse transesterification reaction. This is because a stoichiometric molar ratio of 3:1 is the lowest ratio necessary to lead the reaction toward product formation. The third factor was catalyst loading, with levels of 0.6%, 0.8%, and 1.0%, which were calculated based on the weight of oil used (wt.%). The highest catalyst loading was maintained at 1.0 wt.% since the reaction output is typically prone to gelling due to excessive base catalyst usage.

2.2.4. Sample Characterisation

Gas chromatography (GC) analysis was used to quantify the biodiesel in the post-transesterification products using an Agilent 7820A system. The capillary column utilised was a GL Sciences InertCap WAX-HT column, with an internal diameter of 0.32 mm, length of 30 m, and film thickness of 0.25 μm . During analysis, the carrier gas used was helium, at an oven temperature of 230 $^{\circ}\text{C}$ for a period of 8 min. The internal standard used for the GC analysis was a solution of methyl heptadecanoate (C17:0) dissolved in n-heptane. Samples were prepared by adding the internal standard solution to the post-transesterification products that were extracted and weighed in separate vials. Upon completion of GC analysis, the biodiesel yield was quantified in accordance with EN 14103 standards, following Equation (1):

$$\% \text{Biodiesel} = \frac{\sum A - A_{\text{IS}}}{A_{\text{IS}}} \times \frac{C_{\text{EI}} \times V_{\text{EI}}}{m} \times 100\% \quad (1)$$

where $\sum A$ denotes the total peak area (C14:0 to C24:0), A_{IS} represents the peak area of the internal standard, C_{EI} is the internal standard concentration (mg/mL), V_{EI} denotes the internal standard volume in the sample (mL), and m represents the sample mass (mg).

2.2.5. Experimental Conditions and Results Analysis

A stable laminar flow of reactants was maintained throughout the transesterification reaction, while the T-mixer within the microchannel reactor generated an alternating slug flow of oil and methoxide. The peristaltic pumps were set to flow rates of 15 revolutions per minute (RPMs) for oil and 3.7 RPMs for methoxide, while adhering to the 6:1 methanol to oil molar ratio. These pump settings maintained volumetric flow rates of 0.927 mL/min for oil and 0.250 mL/min for methoxide, which resulted in a 1.177 mL/min combined volumetric flow rate. As for other molar ratio permutations, the pump flow rate configurations were readjusted to match the constant combined volumetric flow rate values.

Controlling and maintaining a stable reaction temperature in a common household microwave is challenging. This is due to the non-uniform temperature distribution caused by the sinusoidal nature of microwave radiations. This challenge was overcome by the following methods:

1. Collecting five consecutive samples for each experimental case, with the reaction time of each vial being 1 min.
2. The surface temperature of each vial was recorded before and after sample collection. The reaction temperature of each vial was the average surface temperature before and after sample collection. This denoted the average temperature during sample collection in each vial.
3. A normalisation technique was utilised to prevent anomalies. A total of nine baseline cases were run on various days throughout the experiment completion period. The biodiesel yields of all 27 cases were normalised against the average biodiesel yield of the total baseline cases. The baseline case had a 6:1 methanol to oil molar ratio,

0.8 wt.% catalyst loading, and 60 °C reaction temperature, representing medium (0) levels of each factor.

The results of the full factorial DOE were analysed using a statistics analytical tool (Minitab version 21.3.1). The combined effects of the experimental factors were conceptualised in the form of 2-dimensional contour plots, and the levels of each factor were optimised to maximise the FAME yield, energy cost for biodiesel production, and environmental effects.

3. Results and Discussion

The effects of experimental factors (catalyst loading, methanol to oil molar ratio, and reaction temperature) on the microwave-assisted transesterification reaction using the PETG microchannel reactor are discussed with regards to its respective levels. The combined effects of the factors are jointly discussed to understand the synergistic interaction between the factors. This section contains optical analysis, regression analysis, and the optimisation of experimental factors and levels with regard to the FAME yield, energy cost of biodiesel production, and environmental effects.

3.1. Optical Analysis

Figure 3 shows the optical analysis of microwave-heated biodiesel production in the PETG microchannel reactor, incorporating quantification of slug flow. Three experimental cases were considered, having varied reaction temperatures (50 °C, 60 °C, 70 °C) while maintaining a constant methanol to oil molar ratio of 3:1 and catalyst loading of 1.0 wt.%. Slug flow was analysed during the slug formation phase, within the first 10 s of the microwave-assisted transesterification reaction.

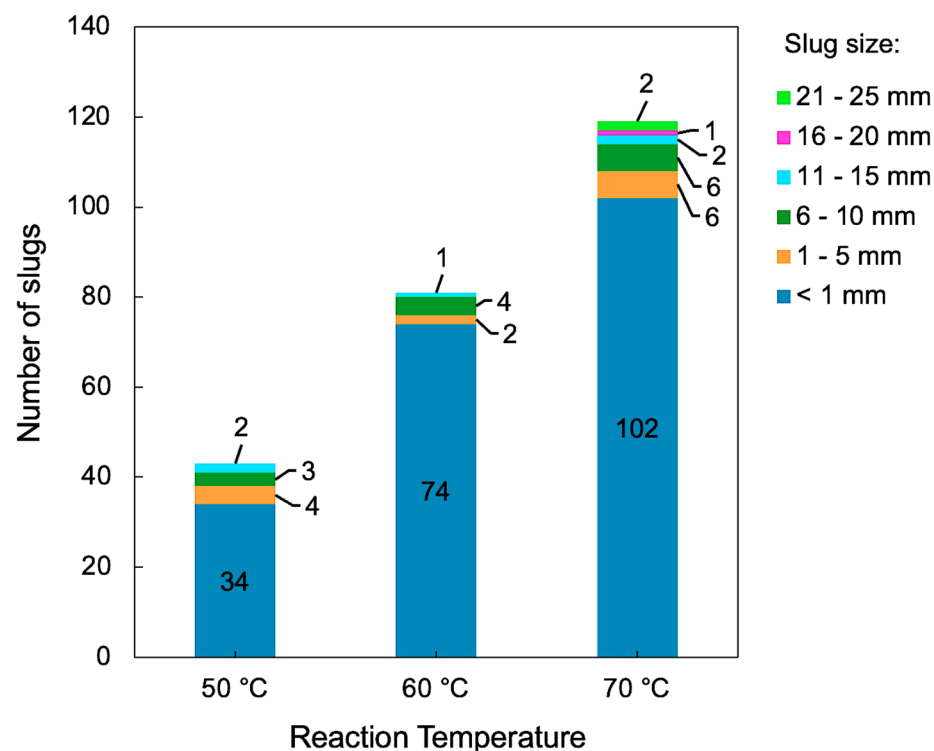


Figure 3. Quantified slug flow via optical analysis of microwave-assisted biodiesel production in the PETG microchannel reactor at 50, 60, and 70 °C reaction temperatures (catalyst loading: 1.0 wt.%, methanol to oil molar ratio: 3:1).

Slugs were grouped based on slug length within the microchannel reactor. During the increase in reaction temperature from 50 to 70 °C, a significant difference in slug quantity was observed for slug lengths below 1 mm compared to other slug lengths. In addition, it

could be noted that the case of 70 °C (Figure 4) was observed to incorporate the highest number of slug length groups, which included slug lengths beyond 15 mm. The increased number of slugs indicated elevated contact between oil and alcohol within the microchannel interfacial area. The increased contact between reactants induced superior mixing effects through internal recirculation zones in between slugs, thus contributing to rapid and complete transesterification reaction. This aligned with the 41.8%, 59.7%, and 100% FAME yields achieved by the 50, 60, and 70 °C cases, respectively, at the 3:1 molar ratio and 1.0 wt.% catalyst loading. Similarly, the findings of Laziz et al. [19] on transesterification in a microchannel reactor revealed that a higher number of slugs resulted in an intensified reaction. This was because of passive mixing, induced by the internal recirculation zones of slugs. Also, Verma et al. [20] investigated biodiesel production in a mini serpentine reactor. Determined through optical analysis, the slug flow regime reportedly resulted in the highest biodiesel yield compared to other flow types within the reactor.

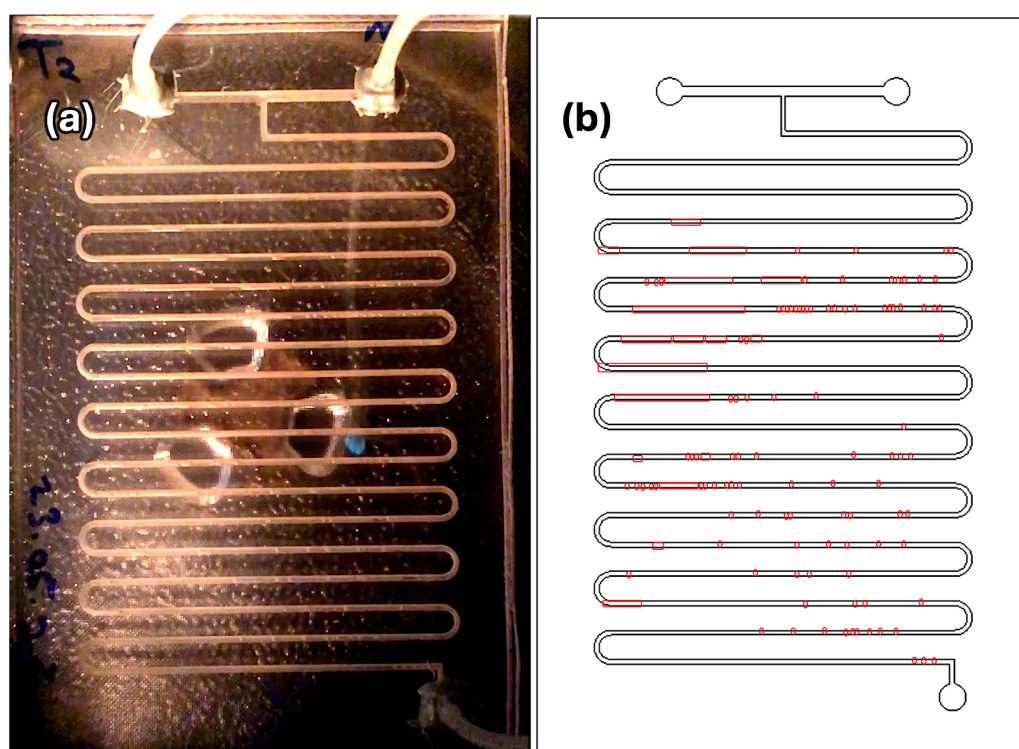


Figure 4. (a) Raw footage and (b) Processed illustration of slug flow via optical analysis featuring microwave-assisted transesterification in the PETG microchannel reactor (reaction temperature: 70 °C, catalyst loading: 1.0 wt.%, methanol to oil molar ratio: 3:1).

3.2. Effects of Reaction Temperature

The influence of reaction temperature on the FAME yield is shown in Figure 5. The catalyst loading varied between 0.6 wt.% and 1.0 wt.% at a fixed methanol to oil molar ratio of 3:1. Overall, increasing the reaction temperature caused the FAME yield to escalate throughout all catalyst loadings. Similar FAME yields were observed for catalyst loadings of 0.6 and 0.8 wt.% at reaction temperatures of 50 °C (28.5% average yield) and 60 °C (39.4% average yield), respectively, with a significantly low yield increment of 10.9% between both temperature ranges. This trend was broken at a reaction temperature of 70 °C, where a separation in FAME yield was observed between 0.6 wt.% (41.8% yield) and 0.8 wt.% (59.7% yield) catalyst loadings. The FAME yields at a catalyst loading of 1.0 wt.% between temperatures of 50 and 60 °C were similar, with an average of 82.9%. A 100% FAME yield was achieved as the reaction temperature increased to 70 °C.

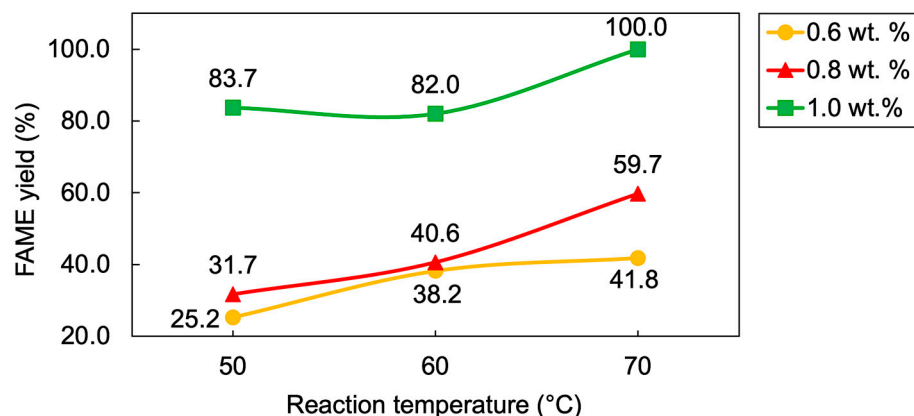


Figure 5. FAME yield at reaction temperatures of 50, 60, and 70 °C (catalyst loadings: 0.6, 0.8, 1.0 wt.%, methanol to oil molar ratio: 3:1).

At catalyst loadings of 0.8 wt.% and 1.0 wt.%, the increase in FAME yield from 60 °C to 70 °C was greater compared to the yield increment between 50 and 60 °C. This corresponded to sufficient heat energy channeled toward the reactants at 70 °C, induced by microwave heating. Methanol possesses the ability to accept microwave heat energy via ionic conduction and dipolar polarisation, as its polar molecules are sensitive to the irradiation. These phenomena directly superheat reactants at a molecular level through localised superheating. Comparatively, a reaction temperature of 70 °C created a pathway for accelerated and complete transesterification reaction, hence highlighting the influence of reaction temperature for biodiesel production. Meanwhile, the poor FAME yields in the case of 0.6 wt.% catalyst loading, despite the 70 °C reaction temperature, as well as the overall leap in yield throughout the 1.0 wt.% catalyst loading cases compared to other catalyst loadings, was due to the influence of catalyst concentration in the reaction mixture.

Maintaining an optimum reaction temperature is important for the transesterification reaction as heat energy is needed to surpass the diffusion barrier between methanol, catalyst, and triglycerides [21]. As a result, adequate kinetic energy is obtained to escalate the rate of mass transfer between reactants, promoting a forward transesterification reaction that produces biodiesel and glycerol as byproducts [22]. In addition, heat energy lowers the viscosity of triglycerides, which improves their miscibility with methanol [23]. This also enhances the mass transfer between reactants, thus increasing the rate at which transesterification occurs.

The FAME yield at excessive temperatures above the boiling point of methanol is postulated to be adversely affected for conventionally produced biodiesel in large vessels. This is because, while boiling, limited methanol in the liquid phase is available for the transesterification reaction [24]. Besides, the presence of bubbles during the boiling of methanol limits contact between methanol and triglycerides, thus compromising the FAME yield [25]. Similarly, a reduction in biodiesel yield was reported by Nayak et al. beyond the optimum reaction temperature due to the formation of bubbles during the boiling of methanol [26]. However, in the case of the PETG microchannel reactor, which is a closed and continuous system, higher reaction temperatures may be beneficial, contradicting findings of open system biodiesel production in large vessels [27]. This is because the boiling of methanol results in turbulence in the flow regime. The turbulent flow aids in better mixing of the reactants within the interfacial area of the microchannel instead of being evaporated in open systems. In the case of this research work, a reaction temperature of up to 80 °C was tested. However, the experiment was unsuccessful due to malfunction of the PETG microchannel reactor caused by overheating.

3.3. Effects of Catalyst Loading

The effects of catalyst loading on the FAME yield are shown in Figure 6, at methanol to oil molar ratios of 3:1, 6:1, and 9:1, while maintaining a 70 °C reaction temperature.

Generally, the increase in catalyst loading was observed to cause the FAME yield to escalate, regardless of the change in methanol to oil molar ratio. This highlights the influence of catalyst loading as an important factor for biodiesel production in the PETG microchannel reactor. From a methanol to oil molar ratio point of view, it is worth noting that cases of the 3:1 molar ratio recorded much higher FAME yields compared to those of 6:1 and 9:1 throughout the range of catalyst loadings. Also, at the methanol to oil molar ratio of 3:1, the FAME yield increased from 59.7% at a catalyst loading of 0.8 wt.% to 100% yield at 1.0 wt.% loading, accounting for a substantial 40.3% increase.

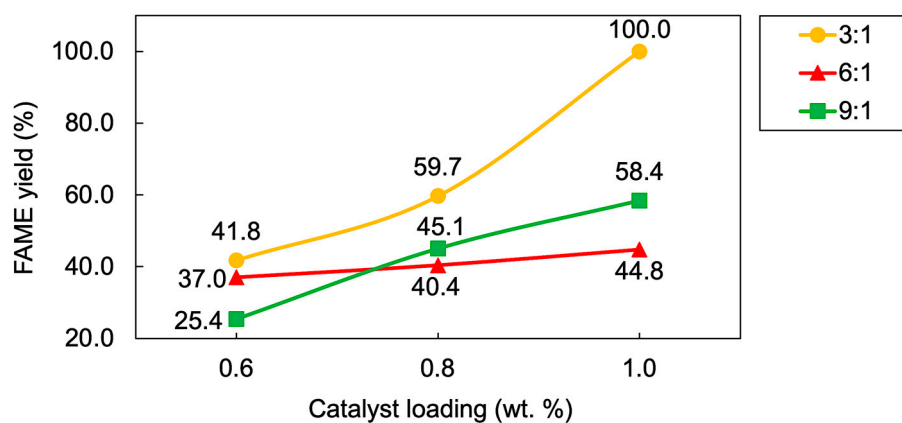


Figure 6. FAME yield at catalyst loadings of 0.6 wt.%, 0.8 wt.%, and 1.0 wt.% (reaction temperature: 70 °C, methanol to oil molar ratios: 3:1, 6:1, 9:1).

The catalyst amount favorably impacts transesterification by reducing the total activation energy needed to commence transesterification reaction. This is because higher catalyst loading relates to an increased number of catalyst active sites present in the reaction mixture [28]. The increase in contact between electrophilic fatty acids in triglycerides alongside the methoxide anion, formed with the base catalyst, decreases the activation energy required, thus accelerating the overall reaction [25]. This explains the incremental trend in FAME yield as catalyst loading increases. The results agreed well with the findings of Zhang et al., where an increase in catalyst loading from 0.2 wt.% to 1.0 wt.% contributed to an increase in biodiesel yield up to 95% [29]. Similarly, Hassan et al. investigated microwave-assisted biodiesel production of waste cooking oil catalysed by potassium hydroxide [30]. The trend in biodiesel yield was reportedly incremental as the catalyst concentration rose between 0.5 wt.% and 1.0 wt.%. Thus, it is crucial to determine the optimum catalyst loading to maximise the FAME yield.

However, it is postulated that a surfeit of base catalyst exceeding optimal amounts diminishes the FAME yield for a variety of reasons. Common backlash includes undesirable formation of soap, where triglycerides react with the base catalyst via the saponification reaction [31]. This adversely affects the FAME yield by limiting the triglycerides available for transesterification, as they are consumed during the saponification reaction. Also, the formation of soap warrants unnecessary time and generates wastewater from biodiesel washing and purification during post-processing [32]. Besides, excessive base catalyst causes the reaction mixture to form an emulsion, eventually developing into a gel [33]. This negatively impacts the FAME yield, as the gel phase significantly increases the viscosity of the post-transesterification products.

The aforementioned postulations are in line with this research work when the catalyst loading was increased to 1.2 wt.%. The PETG microchannel reactor experienced clogging due to the saponification reaction and gelling of the reaction mixture caused by excessive catalyst loading. This disrupted the flow of reactants within the microchannel, ultimately halting product output. Therefore, this suggests that the optimum base catalyst loading for microwave-assisted transesterification in the PETG microchannel reactor is 1.0 wt.%. Similarly, the increase in base catalyst between 1.0 wt.% and 1.5 wt.% evidently diminished

the FAME yield, as reported by Chanthon et al. [34]. This was caused by the formation of an emulsion phase and saponification reaction of palm oil with excessive catalyst.

3.4. Effects of Methanol to Oil Molar Ratio

The influence of methanol to oil molar ratio on the FAME yield is shown in Figure 7 at temperatures between 50 and 70 °C. The overall FAME yield trend was observed to be similar at the various methanol to oil molar ratios across all reaction temperatures. Regardless of the reaction temperature, significantly higher FAME yields were produced at the methanol to oil molar ratio of 3:1, which also recorded the highest FAME yield of 100% at a reaction temperature of 70 °C. Increasing the molar ratio to 6:1 resulted in a steep dip in the FAME yield, in the form of a concave upward pattern. However, a slight increase in yield was observed by further increasing the molar ratio to 9:1. It is worth noting that the change in FAME yield alongside the rise in molar ratio was more distinct as the reaction temperature increased from 50 °C to 70 °C. This highlights the influence of the methanol to oil molar ratio with regard to the reaction temperature.

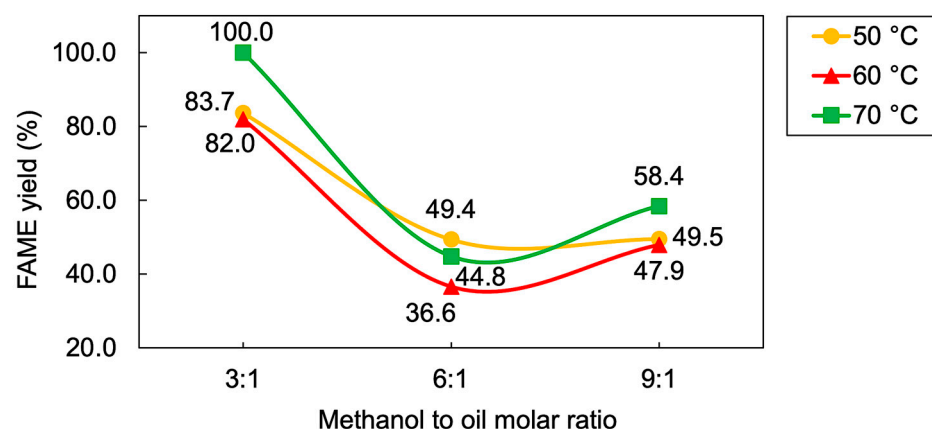


Figure 7. FAME yield at methanol to oil molar ratios of 3:1, 6:1, and 9:1 (catalyst loading: 1.0 wt.%, reaction temperatures: 50, 60, 70 °C).

The FAME yields at temperatures of 50 and 60 °C for molar ratios of 3:1 and 9:1 were similar, with an average of 82.9% and 48.7%, respectively. However, the case of the 6:1 molar ratio had a slight separation in yield, where the cases of 50 °C and 60 °C reaction temperatures achieved yields of 49.4% and 36.6%, respectively. Meanwhile, the case of the 70 °C reaction temperature recorded an 18% higher FAME yield at the 3:1 molar ratio compared to the cases of 50 °C and 60 °C.

A methanol to oil molar ratio of 3:1 is the minimum stoichiometric requirement for biodiesel production. This is because, 3 mols of FAME and 1 mol of glycerol are produced when 3 mols of methanol reacts with 1 mol of triglyceride [34]. Typically, a higher alcohol to oil molar ratio is utilised to direct the transesterification reaction toward product formation for mechanically stirred and conductively heated conventional biodiesel production in large vessels [35]. Transesterification is a reversible process, hence inadequate methanol to oil molar ratios negatively influence the FAME yield, since the reaction rate would be jeopardised for oil conversion [33]. However, the findings of this research work, where the lowest molar ratio of 3:1 was responsible for the highest FAME yield, extraordinarily differ from the trend of conventional biodiesel production, simultaneously highlighting the efficiency of microwave-heated biodiesel production in the PETG microchannel reactor.

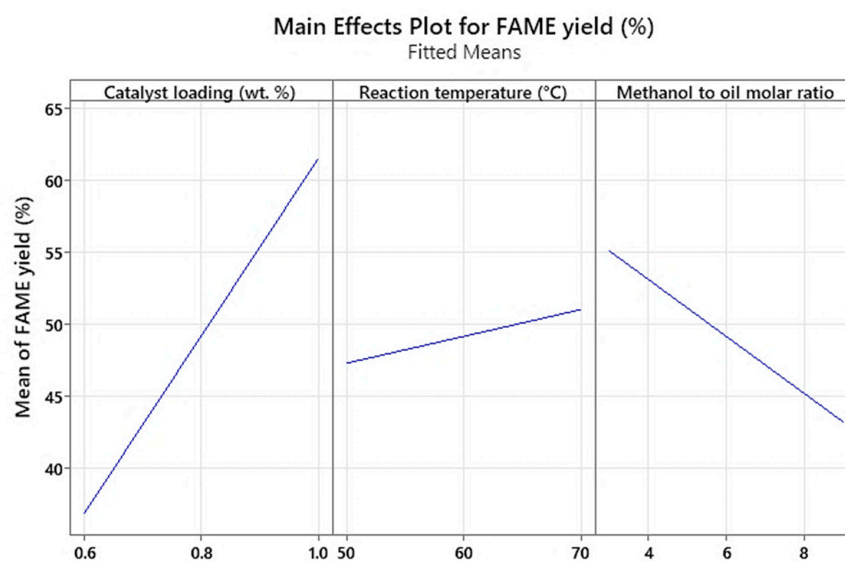
The T-mixer of the microchannel reactor induced alternating slug flow patterns of methoxide and palm oil that elevated contact between both reactants while ensuring enhanced mixing through internal recirculation zones in between the slugs. Micro-scale mixing via slug flow regime eliminated both chemical and physical limitations of transesterification. This accelerated the rate of biodiesel production through elevated mass transfer among reactants. In addition, microwave irradiation ensured direct heat transfer

to the reactants at a molecular level. As a result, the polar molecules of methanol were superheated through the phenomena of dipolar polarisation and ionic conduction [36]. This enhanced the heat transfer between reactants while enabling the transesterification reaction to commence almost instantaneously. The efficient microwave heating prevented heat loss to the environment and surrounding materials in comparison to conventional biodiesel production subjected to conduction heating. The synergic effects of microfluidics and microwave-assisted heating demonstrated the sufficiency of the lowest methanol to oil molar ratio of 3:1 to facilitate 100% biodiesel yield, thus eliminating the need for an increased molar ratio to drive the reaction in the direction of product formation.

Therewithal, the dip in the FAME yield with the increase in the methanol to oil molar ratio from 3:1 to 6:1 can be explained as the adverse effects of having too much methanol in the reaction mixture. In the slug flow regime, excess methanol limited the contact between methanol slugs and sufficient oil slugs within the interfacial area. Since oil slugs were a limiting factor, the FAME yield was negatively influenced, as optimum contact and mixing of reactants were unfulfilled. Likewise, biodiesel produced by Aghel et al. in a micro-sized reactor reportedly experienced a reduction in yield when the methanol to oil molar ratio exceeded optimum amounts due to the reverse transesterification reaction [37]. On the other hand, excess methanol beyond the optimum amount contributed to dilution of the catalyst in the reaction [38]. The reason is that the catalyst loading calculation was dependent on the weight of oil, regardless of the molar ratio. Dilution of the catalyst jeopardised its performance, as the exposure of catalyst active sites to reactants was limited [27].

3.5. Main Effects Plot

The main effects plot shown in Figure 8 provides an overall trend of FAME yield with regard to the experimental factors and corresponding levels. Catalyst loading was the most influential factor for microwave-heated biodiesel production in the PETG microchannel reactor, denoted by the steep gradient of the FAME yield that increased following the escalation of catalyst loading from 0.6 wt.% to 1.0 wt.%. Reaction temperature was the least influential experimental factor due to the gentle inclination of the FAME yield following the rise in temperature from 50 °C to 70 °C. The methanol to oil molar ratio was observed to be inversely proportional to the FAME yield, where the yield decreased as the molar ratio increased from 3:1 to 9:1. This relates to the efficiency of the PETG microchannel reactor in facilitating a complete transesterification reaction at the lowest methanol to oil molar ratio.



All displayed terms are in the model.

Figure 8. Main effects plot for FAME yield (%) with regard to catalyst loading (wt.%), reaction temperature (°C), and methanol to oil molar ratio.

3.6. Combined Effects of Experimental Factors

The effects of individual experimental factors on the FAME yield were discussed in the previous section. Although the analysis of individual factors is important to understand its impact on the transesterification reaction, the combined effects of multiple parameters are equally crucial. The interactive graphical plots of the combined effects provide valuable insight, projecting a holistic view of FAME yield with reference to the synergic interaction between experimental factors and levels. This enables viewing the FAME yield at any level across the experimental factors.

Figure 9 shows the interaction plot of the FAME yield through fitted means. Figures 10–12 represent the combined effects of experimental factors on the FAME yield in the form of two-dimensional contour plots. The hold values maintained were catalyst loading of 0.8 wt.%, reaction temperature of 60 °C, and methanol to oil molar ratio of 6:1, corresponding to the medium (0) levels of each experimental factor. The middling FAME yield range is represented by the light blue and light green colours, while the lowest and highest yield ranges are represented by the dark blue and dark green colours, respectively.

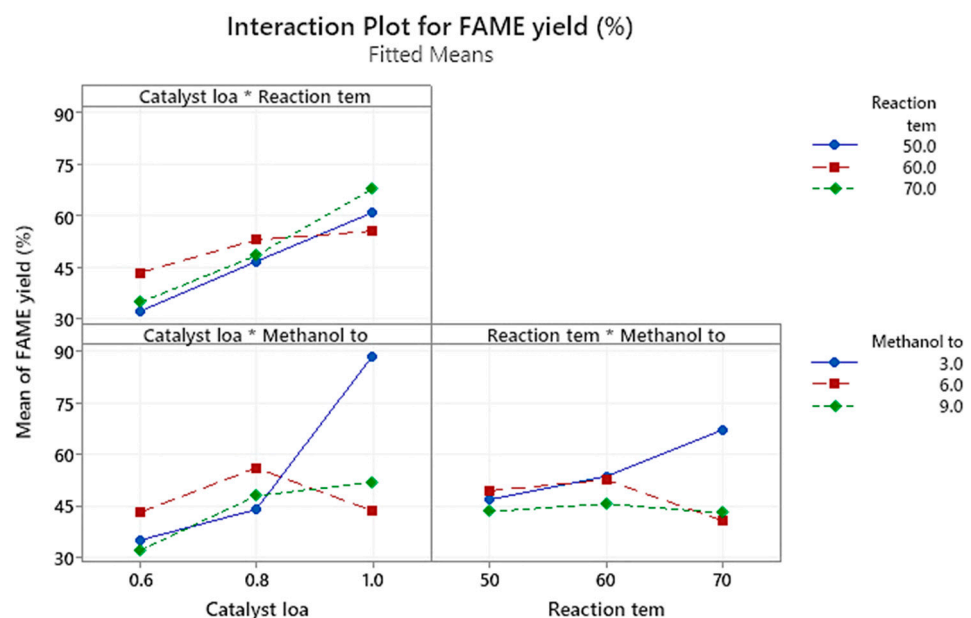


Figure 9. Interaction plot of FAME yield (%) via fitted means. The * symbol denotes interaction between factors.

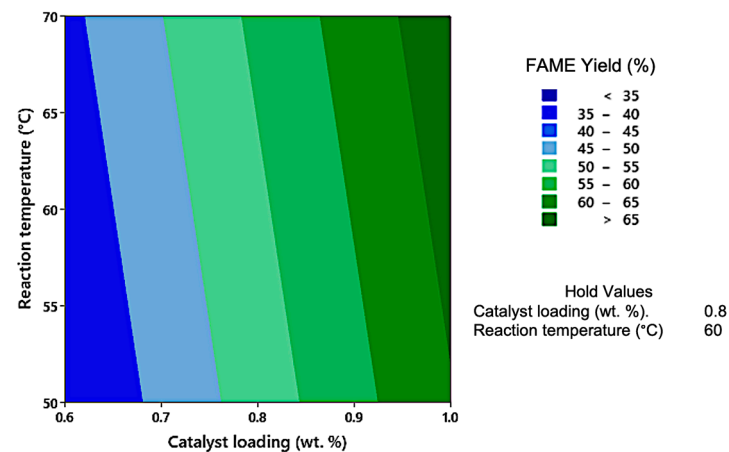


Figure 10. Contour plot representing the combined effects of reaction temperature (°C) and catalyst loading (wt.%) on the FAME yield.

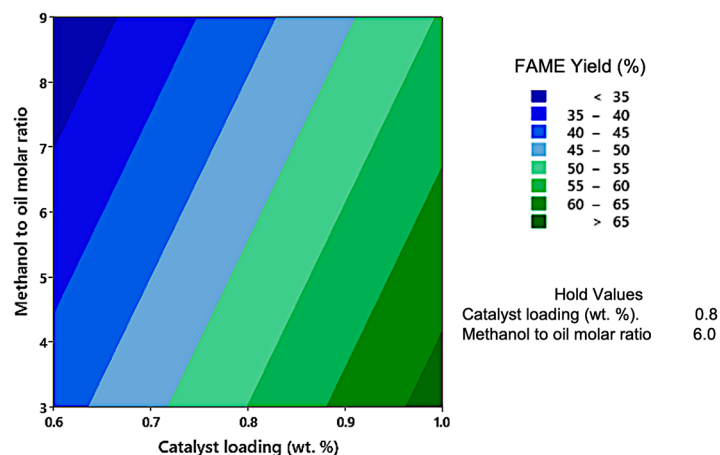


Figure 11. Contour plot representing the combined effects of methanol to oil molar ratio and catalyst loading (wt.%) on the FAME yield.

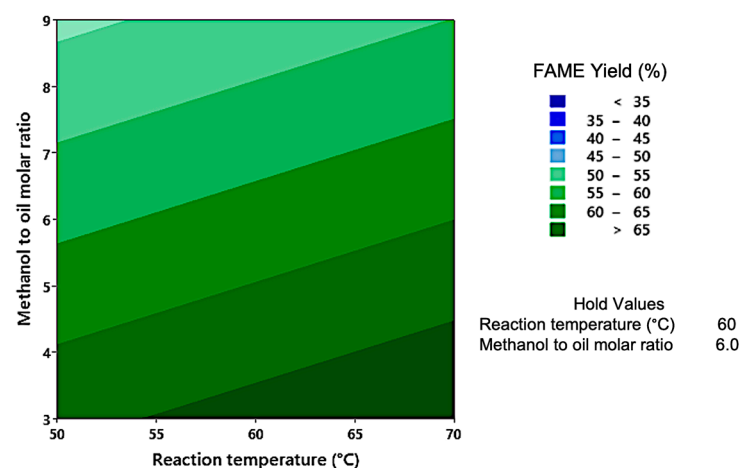


Figure 12. Contour plot representing the combined effects of methanol to oil molar ratio and reaction temperature (°C) on the FAME yield.

The dark blue and dark green colours on the contour plot's legend represent FAME yields of <35% and >65%, respectively, although the best performing experimental case was successful in achieving 100% FAME yield. This is because controlling and maintaining the reaction temperature through microwave irradiation is challenging. Also, small changes in the levels of experimental factors can cause a substantial difference in the FAME yield, induced by microfluidic effects. Both facts generated a wide range of FAME yields across the 27 experimental cases.

3.6.1. Interaction Plot

Figure 9 represents the mean FAME yield through interaction plots of the experimental factors. The interaction between catalyst loading and reaction temperature was directly proportional. However, the increase in FAME yield from catalyst loadings of 0.8 to 1.0 wt.% at a 60 °C reaction temperature was less pronounced compared to all other cases.

The interaction between catalyst loading and methanol to oil molar ratio indicated an increase in the mean FAME yield between catalyst loadings of 0.6 wt.% and 0.8 wt.% across all methanol to oil molar ratios. Between catalyst loadings of 0.8 and 1.0 wt.%, the cases of the 6:1 molar ratio experienced a deterioration in mean FAME yield, indicating 0.8 wt.% catalyst loading as the optimum level. On the other hand, the cases of the 9:1 molar ratio showed an increase in mean FAME yield. However, the cases of the 3:1 molar ratio highlighted that catalyst loading had the greatest influence on transesterification, indicated

by a leap in the mean FAME yield from 45% to about 90%. This was due to accelerated biodiesel conversion through the increase in the number of catalyst active sites.

As for the interaction between reaction temperature and methanol to oil molar ratio, the FAME yield in the case of the 9:1 molar ratio was observed to be insensitive to the effects of reaction temperature, as indicated by the constant mean FAME yield of about 45%. As for the cases of the molar ratio of 6:1, the FAME yield slightly increased between reaction temperatures of 50 to 60 °C, followed by a drop to about 45% when approaching 70 °C. This was due to the adverse effects of excessive methanol in the reaction mixture. As for the cases of the 3:1 molar ratio, the FAME yield increased with the increase in reaction temperature from 50 to 70 °C, indicating the favourable influence of reaction temperature at an optimum molar ratio.

3.6.2. Combined Effects of Reaction Temperature and Catalyst Loading

Figure 10 shows the contour plot illustrating the trend in FAME yield, influenced by the combined effects of reaction temperature (°C) on the y-axis and catalyst loading (wt.%) on the x-axis. FAME yield was poor (<35%) at the low catalyst zone of 0.6 wt.% regardless of the change in reaction temperature. The FAME yield was observed to improve at the middling zone where catalyst loading was 0.8 wt.%. The trend on the contour plot shows that the rise in catalyst loading from 0.6 to 1.0 wt.% at a given reaction temperature promoted a favourable impact on the FAME yield. The FAME yield further escalated, achieving up to 100% yield while approaching the high catalyst zone, peaking at 1.0 wt.% loading. This was attributed to the elimination of heat and mass transfer barriers between reactants via microwave-heated biodiesel production in the PETG microchannel reactor. Comparatively, the results from this research work are superior to those of the study by Joshi et al., who reported 88% yield with 1.0 wt.% base catalyst loading [39].

The catalyst is an influential factor for microwave-heated biodiesel production in the PETG microchannel reactor. Sodium hydroxide catalyst was dissolved in methanol, forming alkoxide ions. During the transesterification reaction, the stepwise transformation of ester and glycerol from triglycerides, diglycerides, and monoglycerides is accelerated by the alkoxide ions of the catalyst [40]. However, a further increase in catalyst loading would result in excess amounts of catalyst in the reaction mixture. It is postulated that excess catalyst would promote the saponification reaction with oil, causing an adverse effect on the reaction equilibrium due to the alkaline nature of the base catalyst. This is in line with the findings of Nayak et al., where excess base catalyst loading beyond 1.0 wt.% resulted in saponification of feedstock (oil), which negatively impacted the FAME yield [26]. Likewise, biodiesel production was negatively affected in this investigation following an escalation of catalyst loading to 1.2 wt.%. The experimental output was subjected to gelling that clogged the PETG microchannel reactor. This disrupted the flow of reactants, eventually ceasing the continuous flow of the transesterification reaction.

As for the reaction temperature, the FAME yield was observed to increase as the temperature increased from 50 °C and peaked at 70 °C. This was due to ionic conduction and dipolar polarisation induced by the microwave onto the reactants at an optimum level. However, high reaction temperature alone was inadequate to produce FAMES in high yield. This was evident in the contour plot, where at a reaction temperature of 70 °C, high catalyst loading was also required to produce high FAME yield. This shows the interaction between the combined effects of reaction temperature and catalyst loading.

Temperatures exceeding 70 °C are postulated to deteriorate the FAME yield, since extreme reaction temperatures degrade FAMES through oxidation and cracking [40]. Nevertheless, higher reaction temperatures up to 80 °C were attempted in this research work. However, the trial resulted in the failure of the PETG microchannel reactor. This may have been due to overheating of the PETG material through excessive microwave energy.

Overall, low reaction temperature and low catalyst loading were unfavourable to producing FAMES in high yield due to the limitations of heat energy and alkoxide ions, respectively. The optimal conditions for achieving the best FAME yield were a high

catalyst loading of 1.0 wt.% and high reaction temperature of 70 °C. This agreed well with the findings of Marwaha et al., where the increment of catalyst loading and reaction temperature to optimal levels reportedly increased the transesterification reaction rate while simultaneously reducing the viscosity of the post-reaction output [41]. In addition, the 100% FAME yield zone of the contour plot was well above the 96.5% yield mark, thus meeting the EN 14214 biodiesel standard.

3.6.3. Combined Effects of Catalyst Loading and Methanol to Oil Molar Ratio

Figure 11 shows the combined effects of catalyst loading (wt.%) and methanol to oil molar ratio on the FAME yield, including the experimental factor levels that maximise the FAME yield. Based on the contour plot, the higher the methanol to oil molar ratio, the lower the FAME yield. In other words, the highest FAME yield of 100% was achieved at the lowest methanol to oil molar ratio of 3:1. This trend was counterintuitive, as higher molar ratios are typically required to drive the transesterification reaction toward product formation, in agreement with Le Chatelier's principle. However, the high FAME yield achieved at the 3:1 molar ratio may have been due to the ease of methoxy ion formation in the PETG microchannel reactor influenced by the effects of microfluidics and microwave irradiation, thus promoting rapid production of biodiesel [26].

On the other hand, the FAME yield was observed to rise as the catalyst loading increased from 0.6 wt.% and peaked at 1.0 wt.%. However, the FAME yield remained poor at lower catalyst loadings despite low molar ratios, which was supposed to escalate the FAME yield with regard to this study. This proved the interdependency between catalyst loading and methanol to oil molar ratio, as the optimal levels of both factors are required to produce 100% FAME yield. The poor FAME yield at the joint permutation of low methanol to oil molar ratio and low catalyst loading was caused by insufficient catalyst concentration in the reaction mixture to complete the transesterification reaction [42]. Beyond a catalyst loading of 1.0 wt.%, it is postulated that transesterification would be adversely affected by undesired emulsification and saponification, complicating product separation and diminishing the FAME yield, respectively [43]. Similarly, Muthukumaran et al. reported complications in the separation of biodiesel induced by excess catalyst concentration [44].

As a whole, neither low catalyst loading nor high methanol to oil molar ratio promoted high biodiesel production in the PETG microchannel reactor. The optimal reaction conditions that resulted in 100% FAME yield were 1.0 wt.% high catalyst loading and the low 3:1 methanol to oil molar ratio. Hence, the contour plot well showcased the interaction trend between catalyst loading and methanol to oil molar ratio in enhancing the FAME yield.

3.6.4. Combined Effects of Reaction Temperature and Methanol to Oil Molar Ratio

The combined influence of reaction temperature (°C) and methanol to oil molar ratio on the FAME yield is shown in Figure 12. The FAME yield was influenced by the reaction temperature, where the yield increased with the rise in temperature from 50 °C to 70 °C. This agreed well with the findings of Marwaha et al., where the increase in reaction temperature at a stipulated molar ratio positively influenced the methyl ester yield due to the increase in rate of reaction [41]. Concerning the molar ratio, the reduction in methanol to oil molar ratio across the range resulted in the escalation of FAME yield. The best molar ratio was observed to be 3:1, which was the lowest level experimented.

The findings of this research contradict with those of other studies, especially pertaining to the trend in the methanol to oil molar ratio. This proves that the effects of microfluidics affect the behaviour of the methanol to oil molar ratio in the PETG microchannel reactor. The decrease in FAME yield beyond the 3:1 molar ratio may have been due to the dilution of the catalyst concentration. Besides, the surfeit of methanol may have caused emulsification of the output, jeopardising the FAME yield, as similarly reported by Verma et al. [45] and Dwivedi et al. [46].

Altogether, the highest FAME yield in the PETG microchannel reactor was achieved by the highest 70 °C reaction temperature and the lowest 3:1 methanol to oil molar ratio, denoted by the darker green zone on the contour plot. The achievement of high FAME yield with the lowest methanol to oil molar ratio creates a pathway for reduced chemical usage, thus lowering the overall production costs of biodiesel.

3.7. Regression Analysis

Regression analysis was conducted to determine the predictor equation of microwave-heated biodiesel production in the PETG microchannel reactor. The analysis initially included all model terms (experimental factors), where the predicted R^2 was 18.24%. However, reaction temperature was highly insignificant, with a p -value of 0.6. This aligned with the main effects plot in Section 3.5, where reaction temperature was found to be least influential on FAME yield.

Hence, the regression analysis was simplified to two model terms, excluding reaction temperature, as shown in Equation (2). Catalyst loading was significant, with a p -value below 0.05, while methanol to oil molar ratio had a p -value of 0.098. The predicted R^2 was 23.53%, indicating an improvement of the model to predict the FAME yield by excluding temperature.

$$\text{FAME Yield}(\%) = 11.8 + 61.5 \text{ Catalyst loading}(\text{wt.}\%) - 1.98 \text{ Methanol to oil molar ratio} \quad (2)$$

The reaction temperature is a key experimental factor in conventional biodiesel research, as its changes are known to have a notable influence on FAME yield. The ability of the PETG microchannel reactor to successfully facilitate biodiesel production with the exclusion of reaction temperature denotes a scientific discovery. This is because biodiesel production would no longer be an energy-intensive reaction that requires high reaction temperatures, thus differing from conventional biodiesel production methods. In the PETG microchannel reactor, micro-level mixing of reactant slugs through the internal recirculation zones was more crucial as it contributed to rapid and complete transesterification reaction.

3.8. Optimisation of Experimental Factors

The optimisation of experimental factors was conducted via the response optimiser function in Minitab statistical software. Optimisation was carried out in the best interest of the FAME yield, production costs, and the environment. The weight and importance of all responses were maintained at 1, while the confidence level for all intervals was 95%.

3.8.1. Optimisation of FAME Yield

Figure 13 shows the optimisation of experimental factors with regard to the FAME yield. The response was optimised to maximise the FAME yield at an upper limit and lower limit of 25.24 and 100, respectively. The experimental factors were catalyst loading of 1.0 wt.%, reaction temperature of 70 °C, and methanol to oil molar ratio of 3:1 for an optimised FAME yield of 69.26% at 58.88% accuracy.

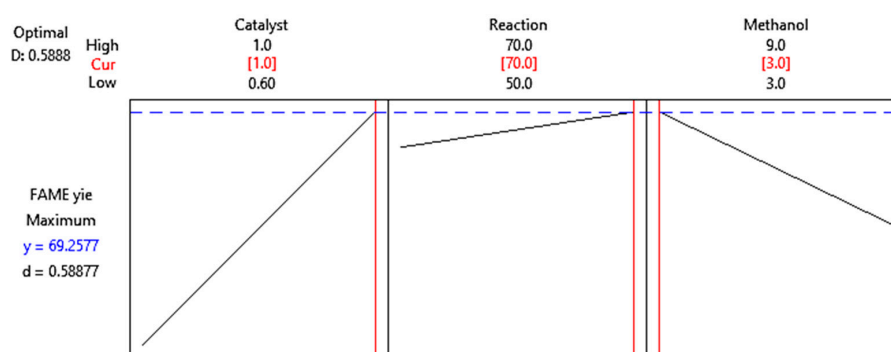


Figure 13. Optimisation of experimental factors with regard to the FAME yield.

The optimised FAME yield was predicted to elevate with the escalation in microchannel length, as its length was directly proportional to the reaction time at a constant reactant flow rate. A longer reaction time would result in increased contact between the reactants and longer exposure to microwave irradiation, thus increasing the FAME yield. In the case of this research work, the length of the PETG microchannel reactor was 1.6 m, which resulted in 69.26% optimised FAME yield. It is postulated that 100% optimised FAME yield could be achieved by increasing the length of the PETG microchannel reactor to 2.3 m.

3.8.2. Composite Optimisation of FAME Yield, Ratio of Energy Cost to Biodiesel Output, and the Environment

Figure 14 shows the composite optimisation of experimental factors with regard to the FAME yield, along with the ratio of energy cost to biodiesel output, and the environment. As for the FAME yield, the response optimiser was set to maximise the FAME yield, similar to that in the previous section.

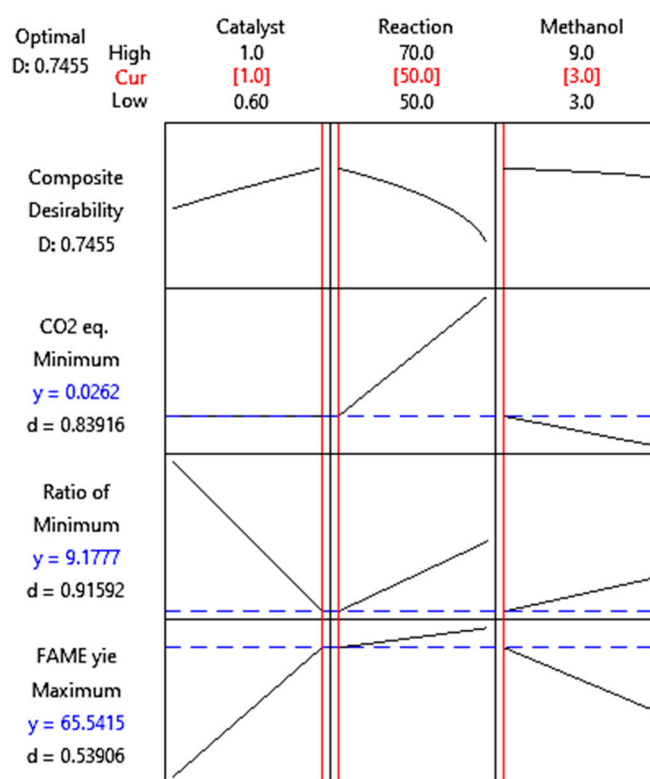


Figure 14. Composite optimisation of experimental factors with regard to the FAME yield, ratio of energy cost to biodiesel output, and the environment.

The ratio of energy cost to biodiesel output was calculated based on the microwave power output (800 W), the externally controlled microwave power on/off cycle during the initial heating (3:1) and sample collection (1:1) phases, the time duration of initial heating (varied according to the relevant reaction temperature), sample collection (1 min), and the Malaysian industrial electricity tariff (35.50 cents/kWh) [47]. The response was set to optimise the outcome by minimising the energy cost for biodiesel output, where the lower limit and upper limit were 7.18 and 30.97, respectively.

The experimental factors were optimised with regard to the environment by representing the reactants and the energy cost for biodiesel production as equivalent (eq.) of carbon dioxide (CO₂) emission. Palm oil, methanol, sodium hydroxide, and electricity were represented by 5.34 kg CO₂ eq./kg palm oil [48], 0.4 kg CO₂ eq./kg methanol [49], 0.6329 kg CO₂ eq./kg NaOH [50], and 0.78 kg CO₂ eq./kWh electricity [51], respectively.

The response was optimised to minimise emissions into the environment, where the lower limit and upper limit were 0.0246 and 0.0349, respectively.

The energy intensity for reactive chemical reactions such as transesterification is considerably high, mainly to maintain the optimal reaction temperature. This relates to elevated production costs and subsequently to a higher carbon footprint with raised emissions. Hence, the composite optimisation was maximised for FAME yield and minimised energy cost for biodiesel output and environmental effects.

The composite optimisation resulted in a catalyst loading of 1.0 wt.%, reaction temperature of 50 °C, and methanol to oil molar ratio of 3:1. The optimised factors of the composite optimisation were more comprehensive than their counterparts solely for maximised FAME yield in Section 3.8.1. This is because the industrial transesterification reaction is collectively influenced by multiple elements, including production costs and environmental effects, apart from the FAME yield. In addition, the lowest reaction temperature of 50 °C through the composite optimisation complemented the regression analysis in Section 3.7 as well as the main effects plot in Section 3.5, where reaction temperature was found to be statistically insignificant.

4. Conclusions

This research work highlights the synergistic effects of microwave heat delivery and microfluidics through the PETG microchannel reactor for biodiesel production. Optical analysis revealed that the presence of a higher number of small slugs below 1 mm in size contributed to accelerated transesterification reaction. A 100% biodiesel yield as per the EN 14214 standards was achieved at a reaction temperature of 70 °C, catalyst loading of 1.0 wt.%, and methanol to oil molar ratio of 3:1. The reaction temperature and catalyst loading were directly proportional to the FAME yield, while the methanol to oil molar ratio was inversely proportional to the yield. The behavioural pattern of transesterification in the PETG microchannel reactor is better understood through the findings of this research, where the lowest methanol to oil molar ratio (3:1) was found to efficiently facilitate the highest biodiesel production, with a yield of 100%. This was made possible through the combination of microwave heating and microfluidics. Microwave heating was responsible for direct heat transmission to the reactants at the molecular scale via ionic conduction and dipolar polarisation of methanol. This enabled the transesterification reaction to begin almost instantaneously while eliminating conductive heat loss, making the process time and energy efficient. Furthermore, the large surface area-to-volume ratio in the PETG microchannel reactor induced a slug flow regime that accelerated the mixing of methanol and vegetable oil through internal recirculation zones and enabled instant separation of byproducts (glycerol) when exiting the microchannel. As a result, microwave-assisted biodiesel production in the PETG microchannel reactor successfully eliminated (1) the heat transmission barrier connecting the heat source to the reactants, and (2) the mass transfer limitation between the reactants, paving a pathway toward energy-efficient and rapid biodiesel production in under 1 min. Meanwhile, microwave-assisted biodiesel production in the PETG microchannel reactor indicated the statistical insignificance of reaction temperature as an experimental factor via regression analysis. This key finding propels future biodiesel research in the direction of low-temperature transesterification. Reducing dependency on the reaction temperature is postulated to suppress the biodiesel production price through lower energy consumption, hence paving the way for wider biodiesel utilisation. Additionally, the composite optimisation of experimental factors with regard to the FAME yield, energy costs of biodiesel production, and environmental effects resulted in a catalyst loading of 1.0 wt.%, reaction temperature of 50 °C, and methanol to oil molar ratio of 3:1. Overall, the novel outcomes of this study promote subsequent research on biodiesel production benefitting from the synergistic effects of microwave heat delivery and micro-level mixing through microfluidics.

Author Contributions: Conceptualization, K.S., J.-H.N. and K.Y.W.; Writing—Original Draft Preparation, K.S.; Writing—Review & Editing, J.-H.N., K.Y.W., K.H.W. and C.T.C.; Visualization, K.S., J.-H.N. and K.Y.W.; Supervision, J.-H.N., K.Y.W. and K.H.W.; Funding Acquisition, J.-H.N. All authors have read and agreed to the published version of the manuscript.

Funding: This research was funded by the Malaysian Ministry of Higher Education (MOHE) through the Fundamental Research Grant Scheme (FRGS) under grant number (FRGS/1/2020/TK0/USMC/02/1).

Data Availability Statement: The data presented in this study are available on request from the corresponding author.

Acknowledgments: The authors thank the Malaysian Ministry of Higher Education (MOHE) and the University of Southampton Malaysia for the support provided.

Conflicts of Interest: The authors declare no conflicts of interest.

References

1. Institute for Energy Research (IER). Fossil Fuels Remain Strong in 2022 Globally, Despite Increases in Renewable Energy. Available online: <https://www.instituteforenergyresearch.org/international-issues/fossil-fuels-remain-strong-in-2022-globally-despite-increases-in-renewable-energy/> (accessed on 25 January 2024).
2. Khan, E.; Ozaltin, K.; Spagnuolo, D.; Bernal-Ballen, A.; Piskunov, M.V.; Di Martino, A. Biodiesel from Rapeseed and Sunflower Oil: Effect of the Transesterification Conditions and Oxidation Stability. *Energies* **2023**, *16*, 657. [CrossRef]
3. Yazdanparast, R.; Jolai, F.; Pishvae, M.S.; Keramati, A. A resilient drop-in biofuel supply chain integrated with existing petroleum infrastructure: Toward more sustainable transport fuel solutions. *Renew. Energy* **2022**, *184*, 799–819. [CrossRef]
4. Ulukardesler, A.H. Biodiesel Production from Waste Cooking Oil Using Different Types of Catalysts. *Processes* **2023**, *11*, 2035. [CrossRef]
5. Cerón Ferrusca, M.; Romero, R.; Martínez, S.L.; Ramírez-Serrano, A.; Natividad, R. Biodiesel Production from Waste Cooking Oil: A Perspective on Catalytic Processes. *Processes* **2023**, *11*, 1952. [CrossRef]
6. García-Martín, J.F.; Barrios, C.C.; Alés-Álvarez, F.-J.; Dominguez-Sáez, A.; Alvarez-Mateos, P. Biodiesel production from waste cooking oil in an oscillatory flow reactor. Performance as a fuel on a TDI diesel engine. *Renew. Energy* **2018**, *125*, 546–556. [CrossRef]
7. Bucciol, F.; Colia, M.; Calcio Gaudino, E.; Cravotto, G. Enabling Technologies and Sustainable Catalysis in Biodiesel Preparation. *Catalysts* **2020**, *10*, 988. [CrossRef]
8. Vakros, J. Biochars and Their Use as Transesterification Catalysts for Biodiesel Production: A Short Review. *Catalysts* **2018**, *8*, 562. [CrossRef]
9. Mushtaq, A.; Hanif, M.A.; Zahid, M.; Rashid, U.; Mushtaq, Z.; Zubair, M.; Moser, B.R.; Alharthi, F.A. Production and Evaluation of Fractionated Tamarind Seed Oil Methyl Esters as a New Source of Biodiesel. *Energies* **2021**, *14*, 7148. [CrossRef]
10. Carlucci, C. An Overview on the Production of Biodiesel Enabled by Continuous Flow Methodologies. *Catalysts* **2022**, *12*, 717. [CrossRef]
11. Yue, Q.; Gao, L.; Xiao, G.; Xu, W. Biodiesel Preparation without a Cosolvent in an Opposite-Side Micro-Fixed-Bed Reactor. *Energies* **2023**, *16*, 4798. [CrossRef]
12. Pavlovic, S.; Selo, G.; Marinkovic, D.; Planinic, M.; Tisma, M.; Stankovic, M. Transesterification of Sunflower Oil over Waste Chicken Eggshell-Based Catalyst in a Microreactor: An Optimization Study. *Micromachines* **2021**, *12*, 120. [CrossRef]
13. Mohd Laziz, A.; Chuah, C.Y.; Denecke, J.; Bilad, M.R.; Ku Shaari, K.Z. Investigation of Mass-Transfer Performance for Biodiesel Reaction in Microchannel Reactor using Volume-of-Fluid with Species-Transport Model. *Sustainability* **2023**, *15*, 6148. [CrossRef]
14. Mohamad Aziz, N.A.; Yunus, R.; Kania, D.; Abd Hamid, H. Prospects and Challenges of Microwave-Combined Technology for Biodiesel and Biolubricant Production through a Transesterification: A Review. *Molecules* **2021**, *26*, 788. [CrossRef] [PubMed]
15. Buasri, A.; Sirikoom, P.; Pattane, S.; Buachum, O.; Loryuenyong, V. Process Optimization of Biodiesel from Used Cooking Oil in a Microwave Reactor: A Case of Machine Learning and Box–Behnken Design. *ChemEngineering* **2023**, *7*, 65. [CrossRef]
16. Lin, C.-H.; Chang, Y.-T.; Lai, M.-C.; Chiou, T.-Y.; Liao, C.-S. Continuous Biodiesel Production from Waste Soybean Oil Using a Nano-Fe₃O₄ Microwave Catalysis. *Processes* **2021**, *9*, 756. [CrossRef]
17. Hsiao, M.-C.; Liao, P.-H.; Lan, N.V.; Hou, S.-S. Enhancement of Biodiesel Production from High-Acid-Value Waste Cooking Oil via a Microwave Reactor Using a Homogeneous Alkaline Catalyst. *Energies* **2021**, *14*, 437. [CrossRef]
18. García, E.; Núñez, P.J.; Caminero, M.A.; Chacón, J.M.; Kamarthi, S. Effects of carbon fibre reinforcement on the geometric properties of PETG-based filament using FFF additive manufacturing. *Compos. Part B Eng.* **2022**, *235*, 109766. [CrossRef]
19. Mohd Laziz, A.; KuShaari, K.; Chin, J.; Denecke, J. Quantitative analysis of hydrodynamic effect on transesterification process in T-junction microchannel reactor system. *Chem. Eng. Process.-Process Intensif.* **2019**, *140*, 91–99. [CrossRef]
20. Verma, R.K.; Ghosh, S. Curvature induced intensification of biodiesel synthesis in miniature geometry. *Chem. Eng. Process.-Process Intensif.* **2021**, *163*, 108363. [CrossRef]
21. Ulakpa, W.C.; Ulakpa, R.O.E.; Eyankware, E.O.; Egwunyenga, M.C. Statistical optimization of biodiesel synthesis from waste cooking oil using NaOH/ bentonite impregnated catalyst. *Clean. Waste Syst.* **2022**, *3*, 100049. [CrossRef]

22. Nazir, M.H.; Ayoub, M.; Zahid, I.; Shamsuddin, R.B.; Zulqarnain; Ameen, M.; Sher, F.; Farrukh, S. Waste sugarcane bagasse-derived nanocatalyst for microwave-assisted transesterification: Thermal, kinetic and optimization study. *Biofuels Bioprod. Biorefining* **2021**, *16*, 122–141. [[CrossRef](#)]
23. Sharma, A.; Kodgire, P.; Kachhwaha, S.S. Investigation of ultrasound-assisted KOH and CaO catalyzed transesterification for biodiesel production from waste cotton-seed cooking oil: Process optimization and conversion rate evaluation. *J. Clean. Prod.* **2020**, *259*, 120982. [[CrossRef](#)]
24. Dehghan, L.; Golmakani, M.-T.; Hosseini, S.M.H. Optimization of microwave-assisted accelerated transesterification of inedible olive oil for biodiesel production. *Renew. Energy* **2019**, *138*, 915–922. [[CrossRef](#)]
25. Yang, J.; Cong, W.-j.; Zhu, Z.; Miao, Z.-d.; Wang, Y.-T.; Nelles, M.; Fang, Z. Microwave-assisted one-step production of biodiesel from waste cooking oil by magnetic bifunctional SrO–ZnO/MOF catalyst. *J. Clean. Prod.* **2023**, *395*, 136182. [[CrossRef](#)]
26. Nayak, M.G.; Vyas, A.P. Parametric study and optimization of microwave assisted biodiesel synthesis from Argemone Mexicana oil using response surface methodology. *Chem. Eng. Process.-Process Intensif.* **2022**, *170*, 108665. [[CrossRef](#)]
27. Hsiao, M.-C.; Kuo, J.-Y.; Hsieh, S.-A.; Hsieh, P.-H.; Hou, S.-S. Optimized conversion of waste cooking oil to biodiesel using modified calcium oxide as catalyst via a microwave heating system. *Fuel* **2020**, *266*, 117114. [[CrossRef](#)]
28. Foroutan, R.; Mohammadi, R.; Esmaeili, H.; Mirzaee Bektashi, F.; Tamjidi, S. Transesterification of waste edible oils to biodiesel using calcium oxide@magnesium oxide nanocatalyst. *Waste Manag.* **2020**, *105*, 373–383. [[CrossRef](#)] [[PubMed](#)]
29. Zhang, M.; Ramya, G.; Brindhadevi, K.; Alsehl, M.; Elfasakhany, A.; Xia, C.; Lan Chi, N.T.; Pugazhendhi, A. Microwave assisted biodiesel production from chicken feather meal oil using Bio-Nano Calcium oxide derived from chicken egg shell. *Environ. Res.* **2022**, *205*, 112509. [[CrossRef](#)] [[PubMed](#)]
30. Hassan, A.A.; Smith, J.D. Investigation of microwave-assisted transesterification reactor of waste cooking oil. *Renew. Energy* **2020**, *162*, 1735–1746. [[CrossRef](#)]
31. Ahmad, T.; Danish, M.; Kale, P.; Geremew, B.; Adeloju, S.B.; Nizami, M.; Ayoub, M. Optimization of process variables for biodiesel production by transesterification of flaxseed oil and produced biodiesel characterizations. *Renew. Energy* **2019**, *139*, 1272–1280. [[CrossRef](#)]
32. Thangarasu, V.; Siddharth, R.; Ramanathan, A. Modeling of process intensification of biodiesel production from Aegle Marmelos Correa seed oil using microreactor assisted with ultrasonic mixing. *Ultrason. Sonochem.* **2020**, *60*, 104764. [[CrossRef](#)] [[PubMed](#)]
33. Kodgire, P.; Sharma, A.; Kachhwaha, S.S. Biodiesel production with enhanced fuel properties via appropriation of non-edible oil mixture using conjoint ultrasound and microwave reactor: Process optimization and kinetic studies. *Fuel Process. Technol.* **2022**, *230*, 107206. [[CrossRef](#)]
34. Chanthon, N.; Ngaosuwan, K.; Kiatkittipong, W.; Wongsawaeng, D.; Appamana, W.; Quitain, A.T.; Assabumrungrat, S. High-efficiency biodiesel production using rotating tube reactor: New insight of operating parameters on hydrodynamic regime and biodiesel yield. *Renew. Sustain. Energy Rev.* **2021**, *151*, 111430. [[CrossRef](#)]
35. Topare, N.S.; Jogdand, R.I.; Shinde, H.P.; More, R.S.; Khan, A.; Asiri, A.M. A short review on approach for biodiesel production: Feedstock's, properties, process parameters and environmental sustainability. *Mater. Today Proc.* **2022**, *57*, 1605–1612. [[CrossRef](#)]
36. Thakkar, K.; Kachhwaha, S.S.; Kodgire, P. A novel approach for improved in-situ biodiesel production process from gamma-irradiated castor seeds using synergistic ultrasound and microwave irradiation: Process optimization and kinetic study. *Ind. Crops Prod.* **2022**, *181*, 114750. [[CrossRef](#)]
37. Aghel, B.; Mohadesi, M.; Razmehgir, M.H.; Gouran, A. Biodiesel production from waste cooking oil in a micro-sized reactor in the presence of cow bone-based KOH catalyst. *Biomass Convers. Biorefinery* **2023**, *13*, 13921–13935. [[CrossRef](#)]
38. Zhu, Z.; Liu, Y.; Cong, W.; Zhao, X.; Janaun, J.; Wei, T.; Fang, Z. Soybean biodiesel production using synergistic CaO/Ag nano catalyst: Process optimization, kinetic study, and economic evaluation. *Ind. Crops Prod.* **2021**, *166*, 113479. [[CrossRef](#)]
39. Joshi, S.; Gogate, P.R.; Moreira, P.F., Jr.; Giudici, R. Intensification of biodiesel production from soybean oil and waste cooking oil in the presence of heterogeneous catalyst using high speed homogenizer. *Ultrason. Sonochem.* **2017**, *39*, 645–653. [[CrossRef](#)] [[PubMed](#)]
40. Jo-Han, N.; Yang, J.K.Y.; Subramaniam, K.; Wong, K.Y.; Chiong, M.C.; Chong, C.T. Microwave-Heated Tubular Reactor for Enhanced Biodiesel Transesterification Process. *Chem. Eng. Trans.* **2023**, *106*, 667–672. [[CrossRef](#)]
41. Marwaha, A.; Rosha, P.; Mohapatra, S.K.; Mahla, S.K.; Dhir, A. Biodiesel production from Terminalia bellerica using eggshell-based green catalyst: An optimization study with response surface methodology. *Energy Rep.* **2019**, *5*, 1580–1588. [[CrossRef](#)]
42. Xiang, Y.; Xiang, Y.; Wang, L. Microwave radiation improves biodiesel yields from waste cooking oil in the presence of modified coal fly ash. *J. Taibah Univ. Sci.* **2018**, *11*, 1019–1029. [[CrossRef](#)]
43. Milano, J.; Ong, H.C.; Masjuki, H.H.; Silitonga, A.S.; Kusumo, F.; Dharma, S.; Sebayang, A.H.; Cheah, M.Y.; Wang, C.T. Physicochemical property enhancement of biodiesel synthesis from hybrid feedstocks of waste cooking vegetable oil and Beauty leaf oil through optimized alkaline-catalysed transesterification. *Waste Manag.* **2018**, *80*, 435–449. [[CrossRef](#)] [[PubMed](#)]
44. Muthukumar, C.; Praniesh, R.; Navamani, P.; Swathi, R.; Sharmila, G.; Manoj Kumar, N. Process optimization and kinetic modeling of biodiesel production using non-edible Madhuca indica oil. *Fuel* **2017**, *195*, 217–225. [[CrossRef](#)]
45. Verma, P.; Sharma, M.P. Comparative analysis of effect of methanol and ethanol on Karanja biodiesel production and its optimisation. *Fuel* **2016**, *180*, 164–174. [[CrossRef](#)]
46. Dwivedi, G.; Sharma, M.P. Application of Box–Behnken design in optimization of biodiesel yield from Pongamia oil and its stability analysis. *Fuel* **2015**, *145*, 256–262. [[CrossRef](#)]

47. Tenaga Nasional Berhad. Industrial Tariff. Available online: <https://www.tnb.com.my/commercial-industrial/pricing-tariffs1> (accessed on 23 December 2023).
48. Schmidt, J.; De Rosa, M. Certified palm oil reduces greenhouse gas emissions compared to non-certified. *J. Clean. Prod.* **2020**, *277*, 124045. [CrossRef]
49. Methanol Institute. Carbon Footprint of Methanol. Available online: https://www.methanol.org/wp-content/uploads/2022/01/CARBON-FOOTPRINT-OF-METHANOL-PAPER_1-31-22.pdf (accessed on 23 December 2023).
50. Thanimalay, L.; Yusoff, S.; Zawawi, N.Z. Life Cycle Assessment of Sodium Hydroxide. *Aust. J. Basic Appl. Sci.* **2013**, *7*, 421–431.
51. Malaysian Green Technology and Climate Change Corporation. Low Carbon Operating System (LCOS) SME Carbon Footprint Snapshot. Available online: <https://www.mgtc.gov.my/lcos-sme-calculator/#:~:text=Electricity%20:%20MY%20Energy%20Commission%202019%20Grid%20EF%20@%200.78%20kgCO2e/kWh> (accessed on 23 December 2023).

Disclaimer/Publisher’s Note: The statements, opinions and data contained in all publications are solely those of the individual author(s) and contributor(s) and not of MDPI and/or the editor(s). MDPI and/or the editor(s) disclaim responsibility for any injury to people or property resulting from any ideas, methods, instructions or products referred to in the content.